Direct Synthesis of Lithium-Intercalated Graphene for Electrochemical Energy Storage Application

Ashavani Kumar,[†] Arava Leela Mohana Reddy,[†,*] Arnab Mukherjee,[‡] Madan Dubey,[§] Xiaobo Zhan,[†] Neelam Singh,[†] Lijie Ci,[†] W. Edward Billups,[‡] John Nagurny,[⊥] Gandhi Mital,[⊥] and Pulickel M. Ajayan[†,‡,*]

[†]Department of Mechanical Engineering and Materials Science and [‡]Department of Chemistry, Rice University, 6100 Main Street, Houston, Texas 77005, United States, [§]U.S. Army Research Laboratory, 2800 Powder Mill Road, Adelphi, Maryland 20783, United States, and [⊥]Lockheed Martin Maritime Systems & Sensors, 9500 Godwin Drive, Manassas, Virginia 20110, United States

ABSTRACT A novel approach for bulk synthesis of lithium-intercalated graphene sheets through the reduction of exfoliated graphene oxide in liquid ammonia and lithium metal is reported. It is demonstrated here that as-synthesized lithiated graphite oxide sheets (Li-RGO) can be directly used as an electrode material in lithium batteries. The electrochemical studies on Li-RGO electrodes show a significant enhancement in the specific capacity of the lithium battery over commercially available graphite electrodes. Partial intercalation of lithium ions in between graphene layers makes this material a good candidate for electrochemical energy storage applications.

KEYWORDS: graphene · liquid ammonia · lithium intercalation · Li-ion battery

Graphene, due to its unique electronic,[1−3] thermal,[4] and mechanical properties,[5,6] has been considered as an ideal material for numerous applications such as field-effect transistors,[7] ultrasensitive sensors,[8] and electromechanical resonators,[9] and recently as an electrode material of Li-ion batteries.[10−12] Various metal oxide−graphene composites have been studied for enhancing capacity and cyclic stability of the Li-ion battery electrodes.[9,11] High-surface-area graphene sheets formed by expanding the spacing between graphene layers have been successfully used for Li-ion battery applications.[12] Various reports on utilizing graphene for energy storage applications confirm its superior electrochemical properties over any other carbon-based materials. However, large-scale synthesis of graphene has been a major issue and presents a considerable challenge of using it in next-generation energy storage devices.

Efforts to develop an efficient synthesis method of graphene include chemical vapor deposition[13] and chemical reduction of exfoliated graphite oxide (GO).[14] Among them, chemical methods are more appealing because of their low cost, scalability, and ease of functionalization. The chemical methods involve reduction of exfoliated graphite oxide using reducing agents such as hydrazine and dimethylhydrazine.[15] Various synthesis methods, such as mild heating of an alkaline solution of exfoliated graphite oxide, complete reduction of graphene through chemical conversion, sodium borohydride and sulfuric acid treatment of graphite oxide, have been reported.[16,17] Although these synthesis methods can be used for the large-scale preparation of graphene, the introduction of impurities during these processes is unfavorable for use in electrochemical devices. Therefore, a synthesis process that would lead to a cleaner product would be desirable. It is known that an alkali metal dissolved in liquid ammonia is a strong reducing agent that can be exploited for the functionalization of carbon-based nanomaterials as well as nanoparticles.[18−22] Billups and co-workers developed a method to functionalize SWNTs using a solution of lithium in liquid ammonia. In this approach, single- or multi-walled carbon nanotubes (SWNT/MWNT) dispersed in Li/NH_3 form "nanotube salts" that react with alkyl or aryl halides to generate free radicals that add to the sidewalls of the nanotubes.[23−25] This method has also been used to attach oxygen- and nitrogen-centered radicals to the sidewalls of the nanotubes.[25] In this paper, we describe a new synthesis method for the preparation of lithium-ion-intercalated graphene sheets and their suitability as an electrode material for lithium ion batteries. The resulting lithium-intercalated reduced graphene oxide (Li-RGO) was used as an electrode material to fabricate a lithium battery and study its electrochemical properties.

* Address correspondence to leela@rice.edu, ajayan@rice.edu.

Received for review October 18, 2010 and accepted May 24, 2011.

Published online May 24, 2011
10.1021/nn201527p

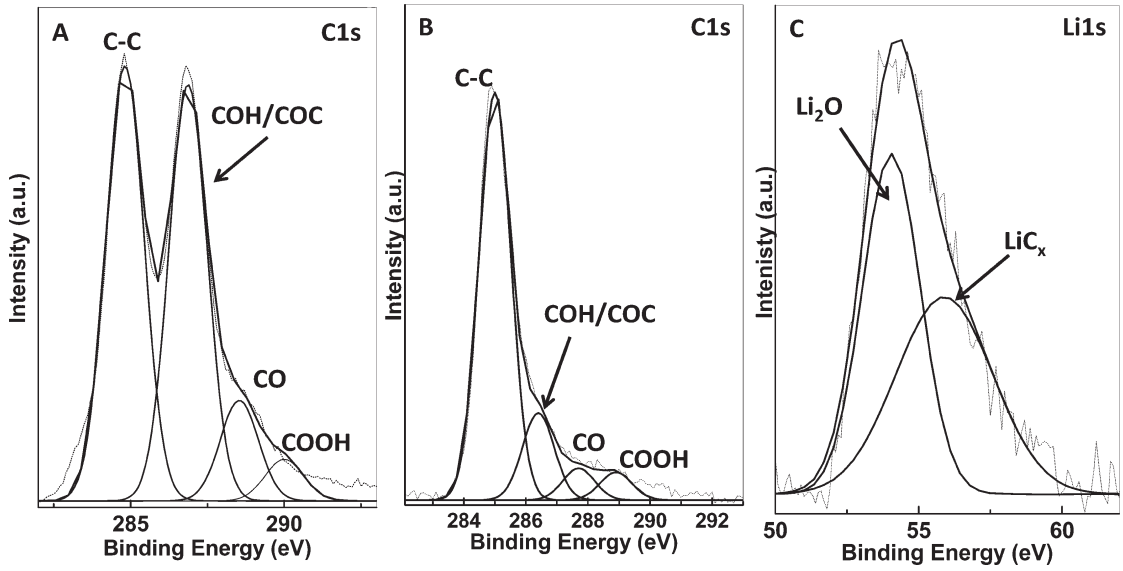

Figure 1. XPS spectra of (A) the C1s core level of graphite oxide, (B) the C1s core level of Li-RGO, and (C) the Li1s core level of Li-RGO.

RESULTS AND DISCUSSION

Characterization of Lithiated Reduced Graphene Oxide. X-ray photoelectron spectroscopy (XPS) studies were conducted in order to determine the presence of surface elements, their oxidation states, and the purity of the as-synthesized material. The survey scan spectrum shows the presence of the principal C1s, O1s, and Li1s core levels with no evidence of impurities. All spectra have been corrected for any background signals using the Shirley algorithm prior to curve resolution.[26] The C1s core level spectra from graphite oxide and lithiated reduced graphite oxide (Li-RGO) are presented in Figure 1A and B, respectively. The C1s peak from graphite oxide can be resolved into four components, centered at ~284.8, 286.9, 288.6, and 290 eV. These components can be assigned to C from nonoxygenated carbon (CC), COC/COH, a carbonyl group (CO), and a COOH group. The intensity of the nonoxygenated *vs* oxygenated carbon clearly indicates that a high degree of oxidation is carried out during the Hummers method.[27] RGO (Figure 1B) also exhibits the same oxygen functionalities that have been assigned for the graphite oxide. However, the peak intensities of these components in Li-RGO samples are much smaller than those in the graphite oxide, indicating that most of the epoxide and hydroxy functional groups are successfully removed by reduction through lithium in liquid NH_3. Figure 1C shows the Li 1s core level spectra and can be resolved into two components, centered at 54 and 57.4 eV, as shown in the figure. The lower binding energy component corresponds to lithium oxide, which may be due to an impurity left in the graphene sample. The higher binding energy component can be assigned to lithium bonded to graphene. The XPS study clearly reveals that graphite oxide has been reduced to graphene oxide with intercalated lithium in between the graphene sheets.

The crystal structure of the synthesized product is analyzed by recording X-ray diffraction (XRD) peaks of the starting, the intermediate, and the final material. Figure 2A shows the XRD data for pure graphite, exfoliated graphite oxide, and reduced graphite oxide (Li-RGO) collected using monochromated Cu Kα radiation. The pure graphite exhibits a sharp peak centered at ~26°, corresponding to the 0002 Bragg reflection. A shift in the 0002 Bragg reflection from ~26° to 10° has been observed in graphite oxide. The shift in the Bragg reflection reveals the successful exfoliation of graphite and is in good agreement with the reported value.[28] The disappearance of the graphite oxide peak at 10° after the reduction process indicates that the oxygen functionality has been removed. Li-intercalated graphene sheets show the peak broadening and shift in the 0002 Bragg reflection toward lower angle (~24°). The broader peak may be due to the corrugated structure of the graphene sheets. The shift of the Bragg reflection toward lower angle clearly indicates the increase in interlayer spacing between graphene layers, which occurred due to partial Li interaction.[29,30]

Raman spectroscopy is an efficient tool to characterize graphene-based materials. Here it is used to monitor the structural changes occurring during the synthesis of Li-RGO from GO. Figure 2B shows the Raman spectra of graphite, exfoliated graphite oxide, and reduced graphite oxide (Li-RGO). The Raman spectrum of the graphite shows a prominent G peak centered at 1581 cm^{-1}, corresponding to the first-order scattering of the E_{2g} mode, whereas the Raman spectrum of graphite oxide shows two peaks, centered at 1594 and 1363 cm^{-1}, which can be attributed to G and D bands, respectively. Similarly, the Li-RGO also

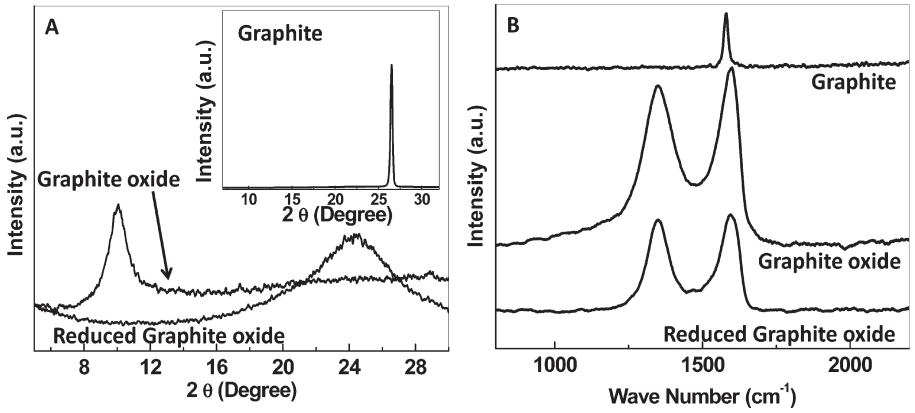

Figure 2. (A) XRD spectra of reduced graphite oxide (Li-RGO), exfoliated graphite oxide, and pristine graphite (inset). (B) Raman spectra of a drop-coated film of pristine graphite, exfoliated graphite oxide, and reduced graphite oxide (Li-RGO).

contains both G and D bands (centered at 1584 and 1352 cm^{-1}, respectively) with a higher D/G intensity ratio as compared to that of GO. This increase in D/G ratio is due to the formation of defects in the graphene layers during reduction of GO and charge transfer between lithium ions and graphene.

The XRD, Raman spectroscopy, and XPS studies clearly indicate the successful reduction of exfoliated graphite oxide into graphene sheets by Li/ammonia treatment. The morphological characterizations of Li-RGO were conducted using SEM and TEM analysis. Figure 3A shows the SEM image of Li-RGO, revealing randomly aggregated, thin, crumpled sheets that form a disordered solid powder with a "fluffy" appearance. In order to see the distribution of Li element in the graphene sheet, energy filter images of graphene sheets are obtained by transmission electron microscopy (TEM) (Figure 3B–D). Figure 3B shows the bright-field image of graphene flakes and is used for chemical mapping. Figure 3C and D show the chemical map of Li and O elements, respectively, indicating the distribution of these elements throughout the graphene sheet.

Electrochemical Studies of Lithiated Graphene. The presence of Li in graphene layers makes this an interesting material for electrochemical studies. In order to test its applicability in energy storage devices, specifically in lithium-ion batteries, a working electrode is prepared by mixing 85% Li-RGO with 10% carbon black and 5% binder (polytetrafluoroethylene). Electrochemical measurements are carried out by taking a 1 M solution of $LiPF_6$ in a 1:1 (v/v) mixture of ethylene carbonate (EC) and dimethyl carbonate (DMC) as the electrolyte and Li foil as counter and reference electrode. Figure 4A shows the cyclic voltammograms (CV) of the Li-RGO electrode conducted at a scan rate of 0.1 mV s^{-1}. The CV measurement of the Li-RGO electrode demonstrates that lithium could reversibly intercalate and deintercalate into graphene sheets. The lithium ion insertion potential is quite low, which is very close to 0 V *vs* the Li/Li^+ reference electrode, whereas the potential for lithium ion deintercalation is in the range 0.2–0.3 V.

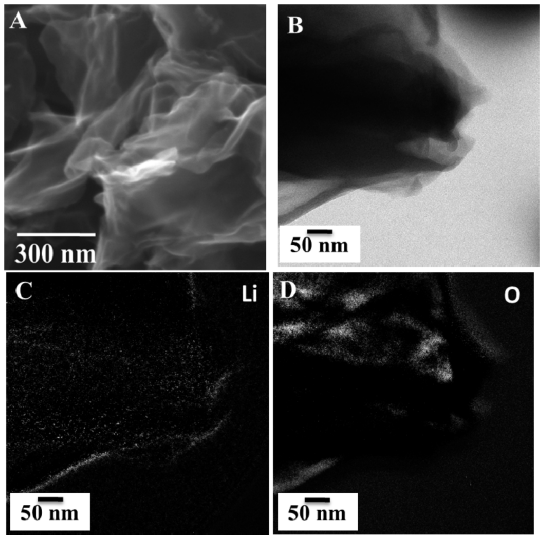

Figure 3. (A) SEM image of Li-RGO, (B) TEM image of Li-RGO, (C) lithium elemental map of Li-RGO, and (D) oxygen elemental map of Li-RGO.

The cyclic stability of the Li-RGO electrodes for lithium ion battery applications is tested by galvanostatic charge/discharge measurements in a Li half-cell at a constant current rate of 25 mA/g. Voltage *vs* specific capacity curves are shown in Figure 4B. The first discharge curve shows a large plateau at about 0.7 V. This discharge plateau can be attributed to the formation of SEI (solid electrolyte interface) film on the surface of the Li-RGO, which is associated with electrolyte decomposition and the formation of lithium organic compounds.[31,32] The discharge plateau at 0.7 V occupies a capacity of ~300 mAh/g and is not reversible. In the subsequent cycles, this discharge plateau disappeared, and a stable reversible capacity of 410 mAh/g was obtained.

A comparison study of the electrochemical cyclic characteristics of the graphite, RGO (prepared by using method described in ref 17), and Li-RGO was conducted at a constant current rate of 25 mA/g between 3.0 and 0.02 V *vs* Li/Li^+. Figure 5 shows the specific

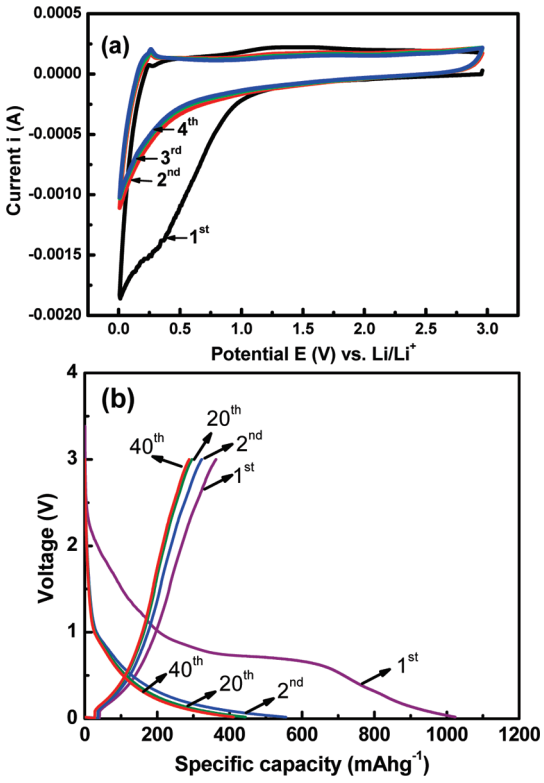

Figure 4. Electrochemical properties of Li-RGO as positive electrodes in the Li battery. (A) Cyclic voltammograms of Li-RGO electrode in a 1 M solution of $LiPF_6$ electrolyte with Li as counter and reference electrode (scan rate: 0.1 mV s^{-1}). (B) Charge−discharge voltage profiles for Li-RGO electrode cycled at a current rate of 25 mA/g between 3.0 and 0.02 V *vs* Li/Li^+ in a 1 M solution of $LiPF_6$ in a 1:1 (v/v) mixture of ethylene carbonate (EC) and dimethyl carbonate (DMC) as the electrolyte.

capacity *vs* cycle number plots for graphite, RGO, and Li-RGO. Graphite, RGO, and Li-RGO show reversible discharge capacities of 300, 340, and 410 mAh/g, respectively. The enhancement in the capacity of Li-RGO as compared to graphite and RGO can be attributed to the presence of electrochemically active defects (*i.e.*, edge and basal-plane defects) formed during the reduction of

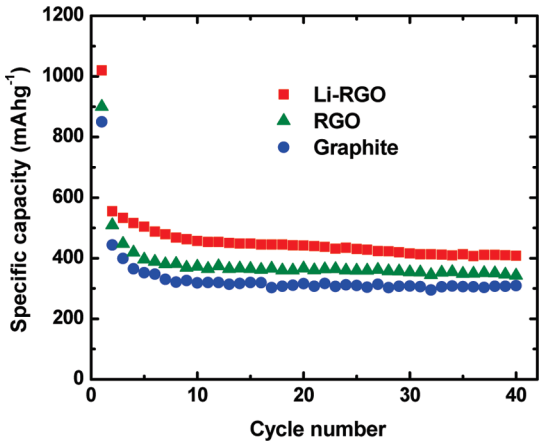

Figure 5. Variation in discharge capacity *vs* cycle number for graphite, RGO, and Li-RGO cycled at a current rate of 25 mA/g between 3.0 and 0.02 V *vs* Li/Li^+ in a 1 M solution of $LiPF_6$ in a 1:1 (v/v) mixture of ethylene carbonate (EC) and dimethyl carbonate (DMC) as the electrolyte.

graphite oxide and also due to the absorption of Li on the internal surfaces of the disordered graphene sheets.[33−35] The interface between liquid electrolyte and the outer surface of each graphene sheet involves SEI formation and results in huge irreversible capacity loss in the first discharge, whereas defects present in the Li-RGO usually undergo a reversible Li intercalation/deintercalation process without involving SEI formation and result in enhanced capacity compared to graphite and RGO.[33]

CONCLUSION

In summary, graphene with intercalated lithium has been synthesized by reducing exfoliated graphite oxide using lithium metal and liquid ammonia. A detailed structural and chemical analysis confirms the simultaneous Li intercalation into graphene sheets upon the reduction of graphite oxide. Electrochemical studies of lithiated graphene reveal its prospect of potential application as an electrode material for Li-ion batteries.

METHODS

Granular lithium (99%), hexane, hydrogen peroxide, and ethanol were purchased from Sigma Aldrich and used as received. Graphite oxide was prepared from purified natural graphite (SP-1, 30 lm nominal particle size, Bay Carbon, Bay City, MI) by the Hummers method.[21] The graphite oxide reduction was carried out as follows: 20 mg (1.6 mmol of carbon) of exfoliated graphite oxide was added to a flame-dried 100 mL, three-neck, round-bottom flask. Liquid NH_3 was then condensed into the flask followed by the addition of small pieces of lithium metal (231 mg, 33 mmol), and the mixture was stirred overnight at −33 °C with slow evaporation of ammonia. The flask was then cooled in an ice bath, and methanol (10 mL) was added slowly followed by slow addition of water (20 mL). After acidification (10% HCl), the reduced product was extracted into hexanes and washed several times with water. The hexane layer was then filtered through a polytetrafluoroethylene membrane filter of 0.2 μm pore size, washed with ethanol, and dried overnight in a vacuum oven (80 °C).

Morphological and elemental analyses were carried out using a scanning electron microscope (FEI Quanta 400) operated at 20 kV and equipped with an EDS detector. The crystalline nature of the products was determined using an X-ray diffractometer (Rigaku D/Max Ultima II) operated at 40 kV using Cu Kα radiation. Transmission electron microscopy (JEOL 2010) was done at 100 kV on drop-casted samples prepared on copper grids. X-ray photoelectron spectroscopy was done on a spectrophotometer (PHI Quantera SXM) using monochromatic Al Kα radiation (1486.6 eV).

Electrochemical measurements were performed in a Swagelok-type cell using an AUTO LAB PGSTAT 302 potentiostat/galvanostat (Eco Chemie Utrecht, The Netherlands). The working electrode with a thickness of 0.2 mm and a diameter of 12 mm was fabricated by mixing 85% of the active materials with

10% carbon black and 5% binder (polytetrafluoroethylene) onto a stainless steel plate. The electrochemical test cell was assembled in an argon-filled glovebox using the active material (Li-RGO, RGO, and graphite powder) as working electrode, lithium metal foil as the counter/reference electrode, and a 1 M solution of $LiPF_6$ in a 1:1 (v/v) mixture of ethylene carbonate and dimethyl carbonate. A glass microfiber filter was used as separator. The cells were charged and discharged galvanostatically at a rate of 25 mA/g between 3.0 and 0.02 V.

Acknowledgment. Financial support from Lockheed Martin is acknowledged. W.E.B. is supported by the Welch Foundation (C-0490). A.L.M.R. thanks the Army Research Office for funding support.

Supporting Information Available: SEM and TEM characterizations of Li-RGO; reaction mechanism of reduction of the graphene oxide; EELS spectra corresponding to Li and C mappings in Li-RGO. This information is available free of charge *via* the Internet at http://pubs.acs.org.

REFERENCES AND NOTES

1. Rutter, G. M.; Crain, J. N.; Guisinger, N. P.; Li, T.; First, P. N.; Stroscio, J. A. Scattering and Interference in Epitaxial Graphene. *Science* **2007**, *317*, 219–222.
2. Tombros, N.; Jozsa, C.; Popinciuc, M.; Jonkman, H. T.; van Wees, B. J. Electronic Spin Transport and Spin Precession in Single Graphene Layers at Room Temperature. *Nature* **2007**, *448*, 571–574.
3. Oostinga, J. B.; Heersche, H. B.; Liu, X. L.; Morpurgo, A. F.; Vandersypen, L. M. K. Gate-induced Insulating State in Bilayer Graphene Devices. *Nat. Mater.* **2007**, *7*, 151–157.
4. Balandin, A. A.; Ghosh, S.; Bao, W.; Calizo, I.; Teweldebrhan, D.; Miao, F.; Lau, C. N. Superior Thermal Conductivity of Single-Layer Graphene. *Nano Lett.* **2008**, *8*, 902–907.
5. Dikin, D. A.; Stankovich, S.; Zimney, E. J.; Piner, R. D.; Dommett, G.H. B.; Evmenenko, G.; Nguyen, S. T.; Ruoff, R. S. Preparation and Characterization of Graphene Oxide Paper. *Nature* **2007**, *448*, 457–460.
6. Stankovich, S.; Dikin, D. A.; Dommett, G. H. B.; Kohlhaas, K. M.; Zimney, E. J.; Stach, E. A.; Piner, R. D.; Nguyen, S. T.; Ruoff, R. S. Graphene-based Composite Materials. *Nature* **2006**, *442*, 282–286.
7. Gilje, S.; Song, H.; Wang, M.; Wang, K. L.; Kaner, R. B. A Chemical Route to Graphene for Device Applications. *Nano Lett.* **2007**, *7*, 3394–3398.
8. Schedin, F.; Geim, A. K.; Morozov, S. V.; Hill, E. W.; Blake, P.; Katsnelson, M. I.; Novoselov, K. S. Detection of Individual Gas Molecules Adsorbed on Graphene. *Nat. Mater.* **2007**, *6*, 652–655.
9. Bunch, J. S.; van der Zande, A. M.; Verbridge, S. S.; Frank, I. M.; Tanenbaum, D. M.; Parpia, J. M.; Graighead, H. G.; McEuen, P. L. Electromechanical Resonators from Graphene Sheets. *Science* **2007**, *315*, 490–493.
10. Wang, D.; Choi, D.; Li, J.; Yang, Z.; Nie, Z.; Kou, R.; Hu, D.; Wang, C.; Saraf, L. V.; Zhang, J.; *et al.* Self-Assembled TiO_2−Graphene Hybrid Nanostructures for Enhanced Li-Ion Insertion. *ACS Nano* **2009**, *3*, 907–914.
11. Paek, S. M.; Yoo, E.; Honma, I. Enhanced Cyclic Performance and Lithium Storage Capacity of SnO_2/Graphene Nanoporous Electrodes with Three-Dimensionally Delaminated Flexible Structure. *Nano Lett.* **2009**, *9*, 72–75.
12. Yoo, E.; Kim, J.; Hosono, E.; Zhou, H. S.; Kudo, T.; Honma, I. Large Reversible Li Storage of Graphene Nanosheet Families for Use in Rechargeable Lithium Ion Batteries. *Nano Lett.* **2008**, *8*, 2277–2282.
13. Malesevic, A.; Vitchev, R.; Schouteden, K.; Volodin, A.; Zhang, L.; Van Tendeloo, G.; Vanhulsel, A.; Haesendonck, C. V. Synthesis of Few-layer Graphene *via* Microwave Plasma-enhanced Chemical Vapour Deposition. *Nanotechnology* **2008**, *19*, 305604–30569.
14. Stankovich, S.; Dikin, D. A.; Piner, R. D.; Kohlhaas, K. A.; Kleinhammes, A.; Jia, Y.; Wu, Y.; Binh, S.; Nguyen, T.; Ruoff, R. S. Synthesis of Graphene-based Nanosheets *via* Chemical Reduction of Exfoliated Graphite Oxide. *Carbon* **2007**, *45*, 1558–1565.
15. Stankovich, S.; Piner, R. D.; Chen, X. Q.; Wu, N. Q.; Nguyen, S. T.; Ruoff, R. S. Stable Aqueous Dispersions of Graphitic Nanoplatelets *via* the Reduction of Exfoliated Graphite Oxide in the Presence of Poly(sodium 4-styrenesulfonate). *J. Mater. Chem.* **2006**, *16*, 155–158.
16. Fan, X.; Peng, W.; Li, Y.; Li, X.; Wang, S.; Zhang, G.; Zhang, F. Deoxygenation of Exfoliated Graphite Oxide under Alkaline Conditions: A Green Route to Graphene Preparation. *Adv. Mater.* **2008**, *20*, 4490–4493.
17. Gao, W.; Alemany, L. B.; Ci, L.; Ajayan, P. M. New Insights into the Structure and Reduction of Graphite Oxide. *Nat. Chem.* **2009**, *1*, 403–408.
18. Liang, F.; Sadana, A. K.; Peera, A.; Chattopadhyay, J.; Gu, Z.; Hauge, R. H.; Billups, W. E. A Convenient Route to Functionalized Carbon Nanotubes. *Nano Lett.* **2004**, *4*, 1257–1260.
19. Sun, L.; Zhang, Z.; Dang, H. A Novel Method for Preparation of Silver Nanoparticles. *Mater. Lett.* **2003**, *57*, 3874–3879.
20. Penicaud, A.; Poulin, P.; Derre, A.; Anglaret, E.; Petit, P. Spontaneous Dissolution of a Single-Wall Carbon Nanotube Salt. *J. Am. Chem. Soc.* **2005**, *127*, 8–9.
21. Borondics, F.; Jakab, E.; Pekker, S. J. Functionalization of Carbon Nanotubes *via* Dissolving Metal Reductions. *Nanosci. Nanotechnol.* **2007**, *7*, 1551–1559.
22. Sumanasekera, G. U.; Allen, J. L.; Fang, S. L.; Loper, A. L.; Rao, A. M.; Eklund, P. C. Electrochemical Oxidation of Single Wall Carbon Nanotube Bundles in Sulfuric Acid. *J. Phys. Chem. B* **1999**, *103*, 4292–4297.
23. Ramesh, S.; Ericson, L. M.; Davis, V. A.; Saini, R. K.; Kittrell, C.; Pasquali, M.; Billups, W. E.; Adams, W. W.; Hauge, R. H.; Smalley, R. E. Dissolution of Pristine Single Walled Carbon Nanotubes in Superacids by Direct Protonation. *J. Phys. Chem. B* **2004**, *108*, 8794–8798.
24. Mukherjee, A.; Combs, R.; Chattopadhyay, J.; Abmayr, D. W.; Engel, P. S.; Billups, W. E. Attachment of Nitrogen and Oxygen Centered Radicals to Single-Walled Carbon Nanotube Salts. *Chem. Mater.* **2008**, *20*, 7339–7343.
25. Mukherjee, A.; Alemany, L. B.; Chattopadhyay, J.; Chakraborty, S.; Guo, W.; Yates, S. M.; Billups, W. E. Dodecylated Large Fullerenes: An Unusual Class of Solids. *Chem. Mater.* **2008**, *20*, 5513–5521.
26. Shirley, D. A. High-Resolution X-Ray Photoemission Spectrum of the Valence Bands of Gold. *Phys. Rev. B: Condens. Mater. Phys.* **1972**, *5*, 4709–4714.
27. Hummers, W.; Offeman, R. Preparation of Graphitic Oxide. *J. Am. Chem. Soc.* **1958**, *80*, 1339.
28. Cai, D.; Song, M. Preparation of Fully Exfoliated Graphite Oxide Nanoplatelets in Organic Solvents. *J. Mater. Chem.* **2007**, *17*, 3678–3680.
29. Celzard, A.; Mareche, J. F.; Furdin, G. Modelling of Exfoliated Graphite. *Prog. Mater. Sci.* **2004**, *50*, 93–179.
30. Lee, S.; Cho, D.; Drzal, L. T. Real-Time Observation of the Expansion Behavior of Intercalated Graphite Flake. *J. Mater. Sci.* **2005**, *40*, 231–234.
31. Frackowiak, E.; Gautier, S.; Gaucher, H.; Bonnamy, S.; Beguin, F. Electrochemical Storage of Lithium in Multiwalled Carbon Nanotubes. *Carbon* **1999**, *37*, 61–69.
32. Aurbach, D.; Ein-Eli, Y. The Study of Li-Graphite Intercalation Processes in Several Electrolyte Systems Using In Situ X-Ray Diffraction. *J. Electrochem. Soc.* **1995**, *142*, 1746–1752.
33. Reddy, A. L. M.; Srivastava, A.; Gowda, S. R.; Gullapalli, H.; Dubey, M.; Ajayan, P. M. Synthesis of Nitrogen-Doped Graphene Films for Lithium Battery Application. *ACS Nano* **2010**, *4*, 6337–6342.
34. Dahn, J. R.; Zheng, T.; Liu, Y.; Xue, J. S. Mechanisms for Lithium Insertion in Carbonaceous Materials. *Science* **1995**, *270*, 590–593.
35. Liu, Y.; Xue, J. S.; Zheng, T.; Dahn, J. R. Mechanism of Lithium Insertion in Hard Carbons Prepared by Pyrolysis of Epoxy Resins. *Carbon* **1996**, *34*, 193–200.